Statistical SPAD Compact Model Dedicated to Pixel Transients Simulations

Jean-Robert Manouvrier†, Denis Rideau†, Gilles Gouget†, Mohammed Al-Rawhani‡, Elsa Lacombe†, Isobel Nicholson‡, Marie BASSET†, Bastien Mamdy†, Raul-andres Bianchi†, Sara Pellegrini‡
†STMicroelectronics Crolles, France.
‡ STMicroelectronics Edinburgh, UK.

***Abstract*— A SPAD (Single Avalanche Photo Diode) Physics based model including all key features to develop and to optimize a pixel design is described in this study. Model Hardware Correlations on Figures of Merits are demonstrated in CMOS technology. The predictability of this model as well as its accuracy and reliability in terms of transient simulations are highlighted.**

Index Terms— SPAD, SPICE, Compact Model, Extraction Flow.

I. Introduction

Currently, there is no SPAD model supported by simulators. Having a SPAD compact model including all key features as Quenching time / DCR (Dark Count Rate) / After pulsing / Pulse width of the Digital Output are key elements to optimize the associated quenching circuit and also the sensor [1]. The SPAD model must take into account mechanisms leading to the breakdown triggering in order to correctly reproduce its behavior during a transient event according to electrothermal conditions [2][3]. Moreover, the models' equations must be the robust enough to prevent convergence issues.

II. Device description

A. Operating mode

As depicted in figure 1, a SPAD is a diode under high reverse biased beyond breakdown voltage (geiger mode) able to generate a breakdown current when a photon is entering the space charge region (noted SCR) (1). Under the high electric field of this Region, the photon energy leads to Hole/Electron pair generation (2). Those free carriers will cross the SCR with a high velocity and will create new free charges due to impact ionization (3). Finally, a breakdown will be generated (4).

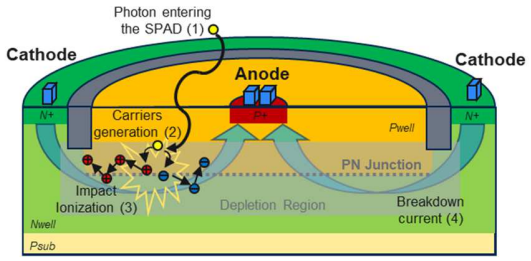

Fig. 1. Simplified sheme of a SPAD during the breakdown triggering from a photon.

III. Modeling

A. Model Scheme

The model is divided into two parts, the optical and electrical. The optical part is composed of a photo generated charges controlled by an optical power source (connected to Light port).

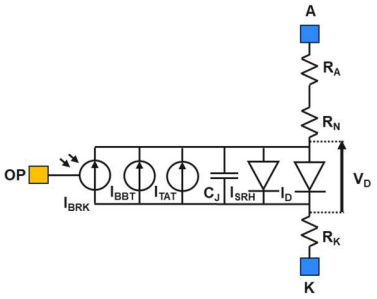

Fig. 2. Equivalent and simplified circuit of SPAD compact model.

The electric part, between the anode (A port) and the cathode (K port), includes constant resistors R_A and R_K due to active regions and interconnects, a modulated resistance, R_N, for low doped region, a junction capacitance C_J. In addition, currents sources in parallel contribute to the total leakage current of the PN junction. A conduction current (I_D), Shockley Read Hall Generation (I_{SRH}), Trap Assisted tunneling (I_{TAT}), band to band tunneling (I_{BBT}) and finally the breakdown current source (I_{BRK}).

B. Physics

1) Breakdown Current generation

First, it's important to have a deep understanding of the key physical mechanisms that lead to SPAD triggering. The breakdown current increases drastically when the impact ionization is strong enough [1]. The generated breakdown current is also described by the current from electrons I and from the holes (h) as :

$$I_{BRK}=I_{BRKe}+I_{BRKh} \quad (1)$$

$$I_{BRKe}=M_e.\ I_e \quad (2)$$

$$I_{BRKh}=M_h\ .I_h \quad (3)$$

Electron–hole pair production due to impact ionization requires a high field strength and the possibility of acceleration in a wide space charge region. If the width of a space charge region is greater than the mean free path between two ionizing impacts, charge multiplication occurs, which can cause electrical breakdown. The reciprocal of the mean free path is called the ionization coefficient. The dimensionless multiplication coefficients $M_{(e,h)}$ depend on the maximum electric field F in the junction according to the Van Overstraeten-de-Man model [4].

$$M_e=\alpha_e.exp[\beta_e/F], \text{ for electrons} \quad (4)$$

$$M_h=\alpha_h.exp[\beta_h/F], \text{ for holes} \quad (5)$$

2) Electric Field

The Maximum Electric Field F (Volt.m^{-1}) in the space charge region is calculated from the charge and the capacitance at zero-biased of the junction, respectively Q_J (Coulomb) and C_{J0} (Coulomb.Volt-1), as well as the Breakdown voltage V_{BRK} (Volt) .

$$F=f_F.Q_J/(C_{J0}.V_{BRK}) \quad (6)$$

The prefactor f_F (Volt.m^{-1}) is introduced to take into account the degradation of the electric field for an excess bias above the breakdown voltage, noted V_{EX}. The function $g(V_{EX})$, not detailed here, is used to degrade the electric field when the excess bias is bigger that a threshold excess, noted V_{EXTH}. Under this threshold, there is no degradation and the fF prefactor is equal to 1.

$$f_F(V_{ex})=1 \text{ for } V< V_{exth} \quad (7)$$

$$f_F(V_{ex})=1/(1+g(V_{ex})) \text{ for } V> V_{exth} \quad (8)$$

$$V_{ex}=V_D-V_{BRK} \quad (9)$$

3) Breakdown voltage

The breakdown voltage depends on the temperature T_{NOM} (K) and is defined by the following equation.

$$V_{BRK}= V_{BRK0}\,(T/T_{NOM})^{(nbrk)} + dV_{BRK} \quad (10)$$

V_{BRK0} (Volt) is the breakdown voltage at the nominal temperature, T_{NOM} equal to 300K, and n_{BRK} is the temperature coefficient. A dynamic variation of the breakdown value, dV_{BRK} , is introduced to take into account the spatial distribution of the breakdown when a photon is entering the SPAD. Thus, this variation is calculated at each time step using a random value of a normal distribution ($rdist_norm veriloga function).

$$dV_{BRK} = \$rdist\_norm(seed, \mu_{DVBRK}, \sigma_{DVBRK}) \quad (11)$$

4) Depletion Charge

The variations of the Electric field with the junction voltage is linked to the junction charge, Q_J, which is defined by this following equation.

$$Q_J=(C_{J0}.pj)/(1-mj).(1-(1-Vd/pj)^{(1-mj)}) \quad (12)$$

C_{J0} (Coulomb/Volt), mj (no unit), and pj (Volt) are respectively the capacitance at zero-biased, the grading coefficient and the built-in potential of the junction.

C. Breakdown trigerring functional diagram

This breakdown source can be triggered if the PN junction is reversed biased beyond the breakdown voltage or if a disruption occurs in the space charge region when the diode is in Geiger mode. If a charge appears in this region under a high electric field, the impact ionization occurs, and the avalanche current is generated.

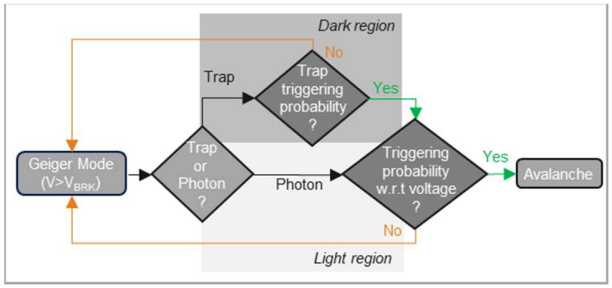

Fig. 3. Breakdown functional diagram.

A hole electron pair can be generated if a photon reaches the SCR (Space Charge Region), it's the photo generation, or if a trap (BBT or SRH) is released from an interface or doping region. This last triggering which leads to an undesired triggering and is directly linked to the dark count rate (noted DCR).

1) Trigerring probability with the bias

When electrical carrier (e/h) is generated in the space charge region, the probability of avalanche triggering is given by the following relation.

$$P_{tr}=1-exp((V_{ex}^{expvex})/(\lambda_{ptr}.V_{BRK})) \quad (13)$$

The avalanche probability is directly linked to the excess bias across the SPAD, noted VPN. The probability of generating an avalanche is lower for an excess voltage around the breakdown voltage and is very high for a higher excess.

2) Traps Trigerring probability

The BBT (Band to Band Tunneling) or SRH (Shockley Read Hall Generation) carriers occur following a pseudo random probability process as depicted in the next figure.

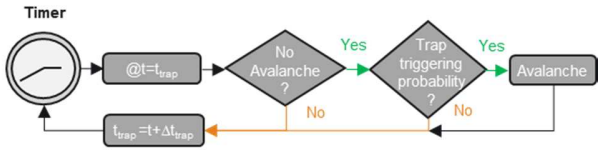

Fig. 4. Dark Triggering from Traps functional diagram.

The time constant and probability parameters are different for each type of carriers and some of them depends on the temperature for the SRH trap. During the transient simulation, a timer is trigger at a time constant which is representative of two

successive traps, noted Δt_{trap}. A dynamic variation of Δt_{trap} is introduced to take into account the random and statistical distribution of this trap release time. This variation is calculated at each time step using a random value of a normal distribution ($rdist_norm veriloga function).

$$\Delta t_{trap} = \$rdist\_norm(seed, \mu_{ttrap}, \sigma_{ttrap})$$

3) Second Trigerring probability

Moreover, the after pulsing effect was also included in this model. This effect is linked to new charge release that leads to a second triggering during the turn off of the first one.

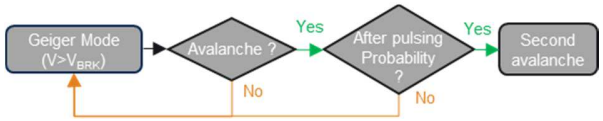

Fig. 5. After Pulsing functional diagram.

IV. Statistical Model Validation at Pixel Level

A. Pixel circuit description

In this study, measurements were performed on the pixel circuit depicted in the figure below.

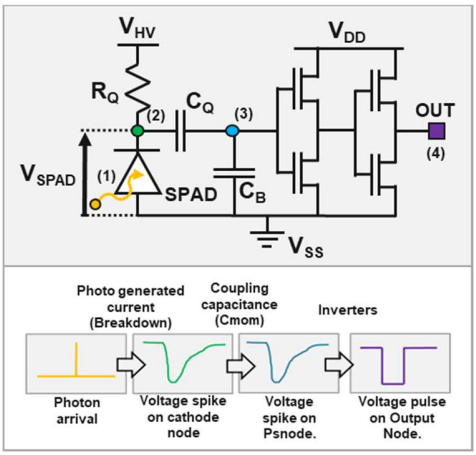

Fig. 6. Simplified pixel circuit with quench circuit and inverters (top) and associated signal processing from photon arrival to digital output.

Dedicated test structures were developed to monitor the spad voltage and current inside the pixel [5]. Then, after the Breakdown voltage and capacitance extraction on DC and AC characterziation, simulations were performed for different seed values in order to refine the statistics parts of the models.

B. Pixel under illumination

Thus, dedicated characterization test structures were developed to monitor the spad voltage and current inside the pixel. Then, a lot of simulations were performed for different seed values for the statistics parts of the models.

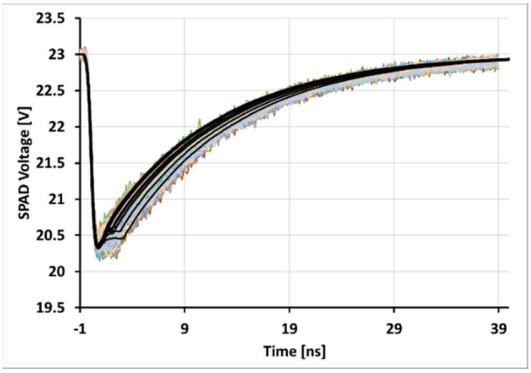

Fig. 7. SPAD Voltage during the triggering for 23V power supply VHV: model hardware correlation between measurements (100 samples, color lines) and Simulations with statistics activated (black lines)

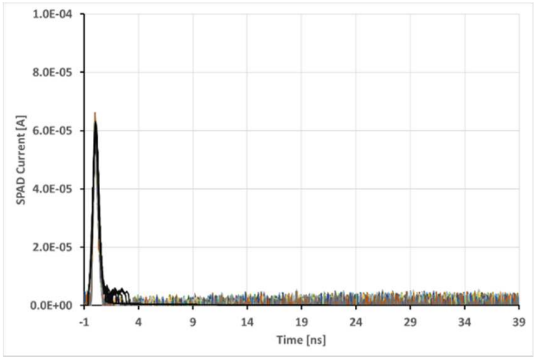

Fig. 8. SPAD Current during the triggering for 23V power supply VHV: model hardware correlation measurements (100 samples, color lines) and Simulations with statistics activated (black lines).

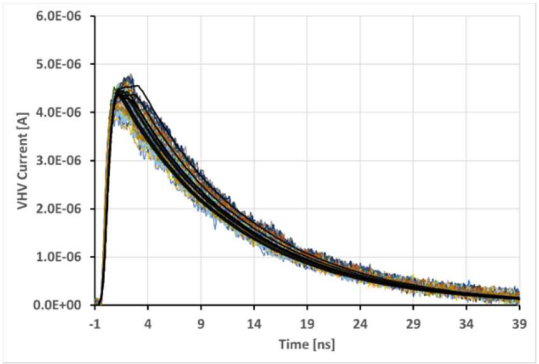

Fig. 9. Current from SPAD power supply during the triggering for VHV 23V power supply: model hardware correlation measurements (100 samples, color lines) and Simulations with statistics activated (black lines).

Then, the after pulsing behavior of the model was validated by comparing the simulations to a measurement sample with a second triggering clearly visible on the SPAD response.

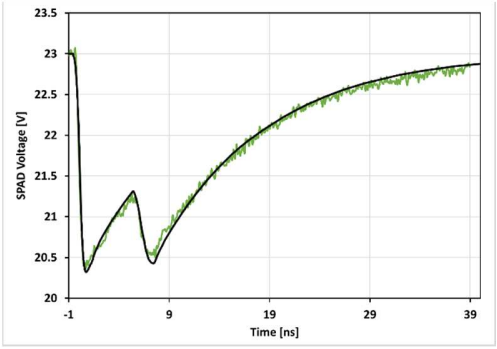

Fig. 10. SPAD Voltage during the triggering for 23V VHV power supply: measurements (green line) and simulations with statistics and after pulsing effect activated (black line).

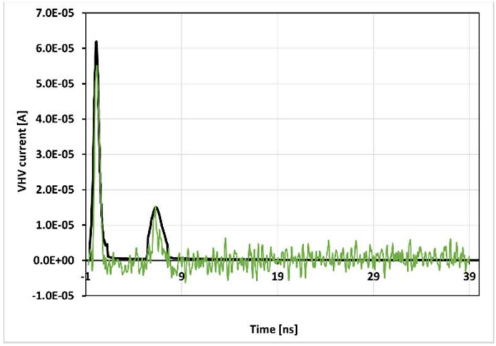

Fig. 11. SPAD Current during the triggering for 23V VHV power supply: measurements (green line) and simulations with statistics and after pulsing effect activated (black line).

Finally, we can also observe that the statistics SPAD model is able to reproduce the stochastic triggering of the SPAD clearly visible on measurements.

C. *Pixel in the dark*

The Dark Count Rate (noted DCR) is measured and simulated without a light source, in the dark, during a long integration time.

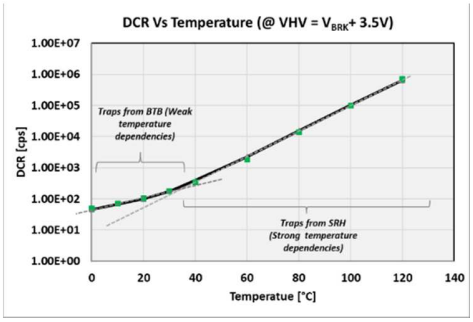

Fig. 12. Dark Count Rate at different temperatures (from 0°C to 120°C) for (VHV= V_{BRK} + 3.5 Volt): Measurements (green squares) and Simulations (black line).

Then, for different value of VHV, we count the number of output pulses generated and we divide by the integration time to have the DCR value in count per second.

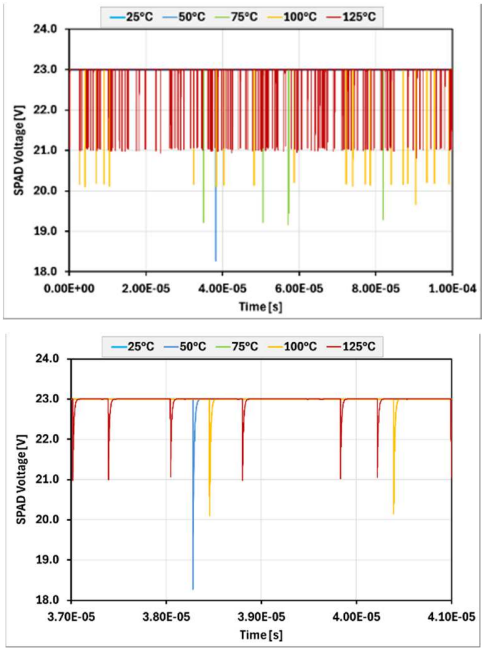

Fig. 13. Simulated SPAD Transient Voltage in the Dark at different temperatures (from 25°C to 125°C) for (VHV=23Volt) from 0 to 100µs (top) and focus between 37µs to 41µs (bottom).

V. Conclusion

In this paper, a Physics based SPAD (Single Photon Avalanche Diode) model including all key features of this device was described. This SPAD model provides a complete coverage of statistical behavior in transient simulations. Its accuracy during the breakdown triggering allows designers to develop and to optimize the SPAD pixel design.

Acknowledgment

Each collaborator of process, characterization, modeling, and design teams are highly acknowledged for their work, their expertise, and their feedback. Thanks to the excellent synergy between teams, a complete and reliable compact model of the SPAD was developed and deployed in our design platforms to provide robust and efficient pixels.

References

[1] D.Rideau et al, “Avalanche build-up field and its impact on the SPAD pulse width and inter-pulse-time distributions.”, 2024 International SPAD Sensor Workshop (ISSW2024)

[2] R. Helleboid, et al. “A Fokker-Planck-based Monte Carlo method for electronic transport and avalanche simulation in single-photon avalanche diodes”, October 2022 , Journal of Physics D: Applied Physics.

[3] D. Rideau, et al. “Single Photon Avalanche Diode with Monte Carlo Simulations: PDE, Jitter and Quench Probability”, 2021 International Conference on Simulation of Semiconductor Processes and Devices (SISPAD), 2021.

[4] R. Van Overstraeten and H. De Man, “Measurement of the ionization rates in diffused silicon p-n junctions,” Solid-State Electronics, vol. 13, no. 5, pp. 583–608, 1970.

[5] D.Rideau, W.Uhring et al, “Direct Measurements and Modeling of Avalanche Dynamics and Quenching in SPADs, September 2023, Conference: ESSDERC 2023 - IEEE 53rd European Solid-State Device Research Conference (ESSDERC).